

CO1-1 Design and Preparation of the Electrode Film for the Study of the Ion Distribution at the Electrochemical Interfaces of Ionic Liquids Using Neutron Reflectometry

N. Nishi and M. Hino¹

Graduate School of Engineering, Kyoto University

¹Research Reactor Institute, Kyoto University

INTRODUCTION: Ionic liquids (ILs), which are liquid salts entirely composed of cations and anions, have potential applications to electrochemical devices because of their several characteristics such as negligible volatility and wide potential window at the IL/electrode interface. The knowledge of the molecular-level structure at IL/electrode interface is important to optimize the performance of the IL electrochemical devices. Theoretical studies have revealed several unique features of the distribution of ions at IL/electrode interface, such as overscreening effect and lattice-saturation effect [1], while experimental studies that shed light on such features are limited to a few. In this study, we aimed to investigate the distribution of ions at the IL/electrode interface using neutron reflectometry. In this report, we will show the results of the design and the preparation of electrode film, which is crucial to sensitively detect the ion distribution.

EXPERIMENTS: To design the electrode material that can be used for the sensitive detection of the ion distribution, neutron reflectivity profile (plot of the neutron reflectivity, R , against the momentum transfer, Q) was simulated for Si/film/IL three phase system. Thin-layer Al-Ti electrode film was prepared on a silicon wafer using a sputter apparatus. For IL, trioctylammonium bis(nonafluorobutanesulfonyl)amide ([TOMA⁺][C₄C₄N⁻]) was prepared from the hydrophilic salts of the IL-constituent ions ([TOMA⁺][Cl⁻] and Li⁺[C₄C₄N⁻]) and purified using column chromatography. Cyclic voltammograms at the [TOMA⁺][C₄C₄N⁻]/film interface were recorded using a three-electrode electrochemical cell. Pt was used as a counter electrode and Ag/AgCl as a quasi-reference electrode.

RESULTS: The calculation of the neutron reflectivity profile revealed that the scattering length density, ρ , of the electrode film strongly affects the sensitivity of the neutron reflectivity profile to the change in the distribution of ions at the IL/electrode interface. Fig. 1 shows an example of the ρ profiles and the neutron reflectivity profiles for Si/film/[TOMA⁺][C₄C₄N⁻] three-phase system when $\rho = 0.8 \times 10^{-6} \text{ \AA}^{-2}$ for the film. One can see that neutron reflectivity profiles are sensitive enough to differentiate three models in which the distribution of TOMA⁺ and C₄C₄N⁻ ions at the electrode/[TOMA⁺][C₄C₄N⁻] interface are different from each other. Such sensitivity to the ion distribution appears when the ρ value of the film is between 0.5 and 1.5 (10^{-6} \AA^{-2}).

To fulfill this ρ condition, we selected Al-Ti alloy as an

electrode material and prepared Al-Ti film on a silicon wafer. The thickness and the composition of Al in the film were evaluated by using x-ray reflectometry to be 46 nm and ~70%, respectively ($\rho \sim 1.0 \times 10^{-6} \text{ \AA}^{-2}$). To confirm the inertness of the film to ILs and to the electric potential change, cyclic voltammograms at [TOMA⁺][C₄C₄N⁻]/film electrode interface were recorded. It was found that the Al-Ti film is inert in [TOMA⁺][C₄C₄N⁻] and has a potential window of at least 1 V.

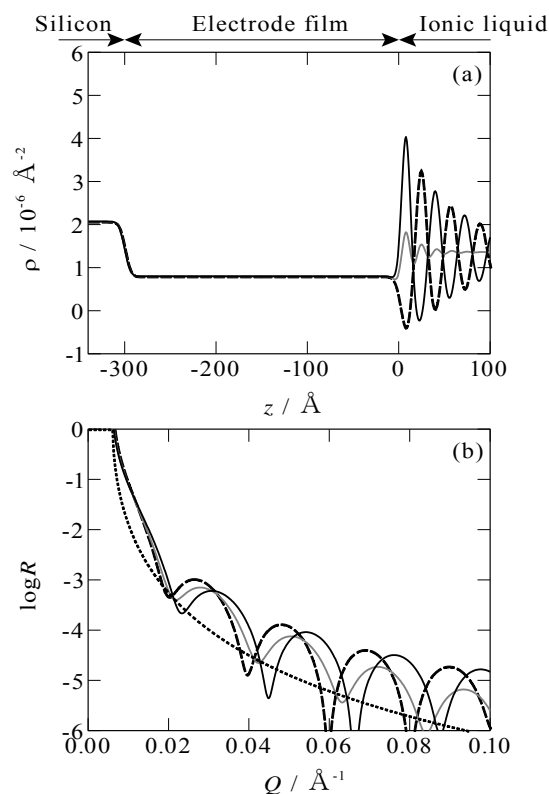


Fig. 1. (a) Scattering length density as a function of z , the displacement along with the surface normal, for Si/film/[TOMA⁺][C₄C₄N⁻] when $\rho = 0.8 \times 10^{-6} \text{ \AA}^{-2}$ for the film. Si, the film and [TOMA⁺][C₄C₄N⁻] are at $z/\text{\AA} \leq -300$, $-300 \leq z/\text{\AA} \leq 0$, $z/\text{\AA} \geq 0$, respectively. (b) Neutron reflectivity as a function of momentum transfer. Solid line is from Anion-topmost ALC model [2], dashed line from Cation-topmost ALC model, gray line from noncharged DCM model [3], and dotted line in (b) is the Fresnel reflectivity.

REFERENCES:

- [1] A. A. Kornyshev, J. Phys. Chem., B 111 (2007) 5545.
- [2] M. Mezger *et al.*, Science, **322** (2008) 424.
- [3] O. M. Magnussen *et al.*, Phys. Rev. Lett., **74** (1995) 4444.

M. Sugiyama, Y. Nishikawa*, K. Mori and T. Fukunaga

Research Reactor Institute, Kyoto University

*Graduate School of Engineering, Kyoto University

INTRODUCTION: Hydrogen is expected to be base of next generation energy in our world. However, there are still problems which should be solved from a practical application perspective. One of them is how to store hydrogen. Hydrogen storage alloy could be expectable candidate for portable hydrogen storage tanks due to its high hydrogen density in unit volume and also in unit weight. Therefore, in these years, many researchers have been improving hydrogen storage performance of alloy, such as hydrogen density in unit volume, in unit weight, plateau temperature and so on. One of difficult problems for improving the performance of hydrogen storage alloy is 'residual hydrogen', which remains in the alloy under the external hydrogen pressure less than that of plateau. In other words, it is considerably effective to reduce an amount of the residual hydrogen to improve an amount of available hydrogen in an alloy. Therefore, we have started to research characteristic feature of hydrogen in alloy to reduce the amount of the residual hydrogen in alloy as a final goal.

Among hydrogen absorbing materials, body centered cubic (bcc) solid solution alloys possess a large hydrogen capacity. For example, Ti-Cr-V bcc alloy transforms into (Ti-Cr-V)₂H₂, which has the CaF₂-type structure (i.e., fcc structure), by the hydrogenation reaction at room temperature (RT). Its hydrogen-to-metal ratio (H/M) is 2.0, compared with 1.1 H/M for LaNi₅H₇ and 1.3 H/M for Mg₂NiH₄. This is the reason why the Ti-Cr-V bcc alloy has attracted much attention as promising hydrogen storage applications such as a hydrogen storage tank of an automobile. However, the detailed hydrogen absorbing mechanism of Ti-Cr-V is still unclear, particularly the surface structure of Ti-Cr-V in the hydrogenation reaction.

The aim of this experimental proposal is to clarify the surface (or interface) structure of the Ti-Cr-V bcc alloy in the hydrogenation reaction, using Small-Angle Neutron Scattering (SANS).

METHOD: For the SANS experiments, we have prepared a null-alloy of Ti_{0.31}Cr_{0.33}V_{0.36} (i.e., b_c ~ 0) in order to enhance the surface (or interface) structure for the hy-

dride samples such as (Ti_{0.31}Cr_{0.33}V_{0.36})H_{1.7}, (Ti_{0.31}Cr_{0.33}V_{0.36})D_{1.7}.

RESULTS: Fig. 1 shows SANS profiles of the hydrogen storage alloy, Ti_{0.31}Cr_{0.33}V_{0.36} and (Ti_{0.31}Cr_{0.33}V_{0.36})D_{1.7}. Hydrogen storage increases the SANS intensity and also changes power of law from -3.0 to -4.0. It is well known that SANS intensity of material which has surface fractal structure is expressed by,

$$I(q) \sim q^{-(6-d)},$$

where d is surface fractal dimension. This result clearly shows that the surface of Ti_{0.31}Cr_{0.33}V_{0.36} becomes smooth by deuterium storage. Now, we are considering the mechanism to make the surface smooth by hydrogen storage.

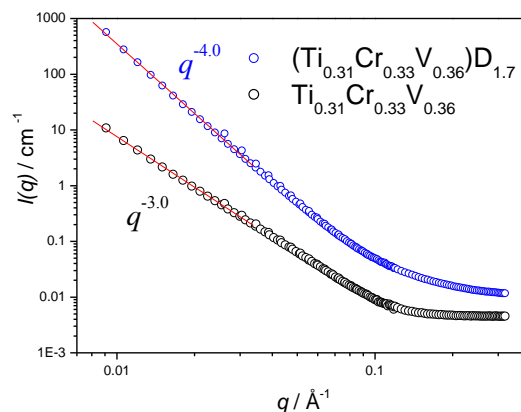


Fig. 1. SANS profiles of the hydrogen storage alloy, Ti_{0.31}Cr_{0.33}V_{0.36} and (Ti_{0.31}Cr_{0.33}V_{0.36})D_{1.7}.

H. Hyodo and T. Itaya

Research Institute of Natural Sciences,
Okayama University of Science

INTRODUCTION: Recent findings of fossils of great apes in the eastern Africa have drawn great attention as their origin seems to have a close correlation to that of human beings [1]. Age determination of these fossils is often difficult simply due to lack of index fossils in the strata or lack of suitable minerals for isotopic dating. The strata often have volcanic ash layers, and the fossils are held between them. Ages of the upper and lower ash layers of such fossil-bearing layers will constrain the age of the fossils. However, technical difficulties also exist in dating volcanic ash using the K-Ar system.

We carried out $^{40}\text{Ar}/^{39}\text{Ar}$ laser step heating experiments to determine ages of volcanic layers containing feldspar minerals.

EXPERIMENTS: Rock samples were crushed, and sieved in #25-50 mesh. After ultrasonic cleaning in distilled water, single mineral grains were handpicked. The minerals were irradiated in the KUR reactor for 24 hours at 1 MW for $^{40}\text{Ar}/^{39}\text{Ar}$ age determination. The total neutron flux was monitored by 3gr hornblende age standard [2], [3], which was irradiated in the same sample holder. In the same batch, CaSi_2 and KAlSi_3O_8 salts were used for interfering isotope correction. A typical J-value of the age standards was $(5.499 \pm 0.022) \times 10^{-3}$. In stepwise heating experiment, temperature of a mineral grain was measured using infrared thermometer whose spatial resolution is 0.3 mm in diameter [4] with a precision of 5 degrees.

RESULTS: An example of age spectra results from stepwise heating experiments were shown in Fig. 1. The first four fractions in the lower temperatures suggest a possibility of a secondary alteration. Preliminary results of other samples also indicate significant alterations confirmed under a microscope. In spite of the alterations, the age spectra consistently show plateau-like fractions at the high temperatures. The age distributions suggest that the timing of the volcanic activity is approximately 20-21 Ma, giving a constraint on the lower limit of the fossiliferous

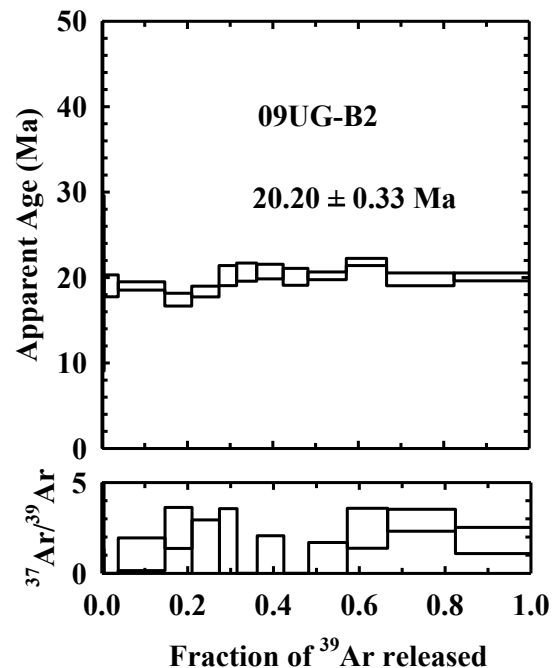


Fig. 1. $^{40}\text{Ar}/^{39}\text{Ar}$ age and $^{37}\text{Ar}/^{39}\text{Ar}$ ratio spectra of a feldspar from volcanic ash strata in Napak, Uganda. The ratio spectra suggest a presence of relatively homogeneous gas release from low to high temperatures. This age and other plateau-like age spectra implies the age of volcanic activity is about 20 Ma.

strata. However, the age of the strata is possibly a few million years younger, considering other geological factors.

REFERENCES:

- [1] Y. Kunimatsu and 13 others (H. Hyodo at the 6th). Proceedings of National Academy of Science **104** (2007) 19220-19225.
- [2] G. Turner, J.C. Huneke, F.A. Podosek and G.L. Wasserburg, Earth Planet. Sci. Lett. **12** (1971) 19-35.
- [3] J.C. Roddick, Geochim. Cosmochim. Acta **47** (1983) 887-898.
- [4] H. Hyodo, S.-W. Kim, T. Itaya and T. Matsuda, J. Min. Petr. Econ. Geol. J. **94** (1999) 329-3.

Y. Arimoto, P. Gertenbort¹, S. Imajo², Y. Iwashita³,
M. Kitaguchi⁴, Y. Seki⁵, H. M. Shimizu⁶, T. Yoshioka⁷

KEK,¹ILL,²Dep. of Phys. Kyoto Univ.,³ICR Kyoto Univ.,
⁴KURRI,⁵RIKEN,⁶Dep. of Phys. Nagoya Univ.,⁷Dep. of
Phys. Kyushu Univ.

INTRODUCTION: The permanent electric dipole moment of neutrons (nEDM) signals the violation of time-reversal (T) invariance. The present upper limit is $|d_n| < 2.9 \cdot 10^{-26} e \text{ cm}$ (90% C.L.) [1], which is very close to the predictions of some physics beyond the standard model of particle physics, for example, supersymmetry. For improvement of experimental sensitivity, the density of neutrons is quite important in order to reduce the systematic errors from the uncertainty of the environment. We are developing the transport system against loss of neutron density. In the case of pulsed neutron source, the neutron pulse with high density spreads spatially and loses the density during transport because of their velocity distribution. When fast neutrons are decelerated and/or slow neutrons are accelerated properly in the middle of the transport, these neutrons can be focused on the experimental area at the same time with recovering the density [2].

EXPERIMENTS: We made the adiabatic fast passage (AFP) spin flipper as the neutron accelerator, which consists of a compact static magnet to generate the gradient field with 1 T at the maximum and an RF coil to generate the resonance RF field (Fig. 1). When a neutron passes through the AFP, the neutron's spin flips with energy gain or loss. The energy can be controlled by selecting the frequency of the RF. The frequency can be synchronized with the neutron pulse. The RF power is supplied by a wideband amplifier with 1 kW output.

The space-time focusing experiment was performed at the PF2 TES beam line in the High Flux Reactor at Institut Laue Langevin. Ultracold neutrons (UCNs) were provided from the turbine, which decelerates the neutrons from the reactor by using continuous reflections off rotating mirrors. A mechanical shutter is used to supply pulsed neutrons. The neutrons were transported with reflections off the mirror inside the guide tube.

RESULTS: We measured the TOF spectrum of the neutrons through this setup. Comparing the cases of RF ON with the case of RF OFF, accelerated and decelerated neutrons can be seen (Fig. 2). The observed histograms are in good agreement with Monte Carlo simulations. Upon further analysis, the focusing of UCNs has been confirmed. The efficiency of the spin flip was low, however, this can be improved with the amplitude of the RF field.

The combination of this device and an intense pulsed source, for example, SNS and J-PARC, enable us utilize neutrons most effectively. We are planning the new nEDM experiment using this focusing technique and the new type of magnetometers with extremely high precision.

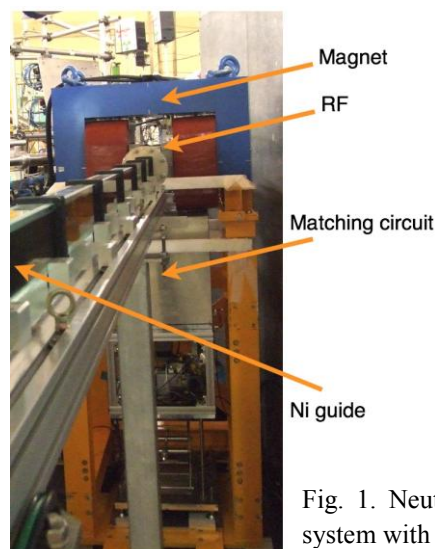


Fig. 1. Neutron accelerator system with magnet and RF.

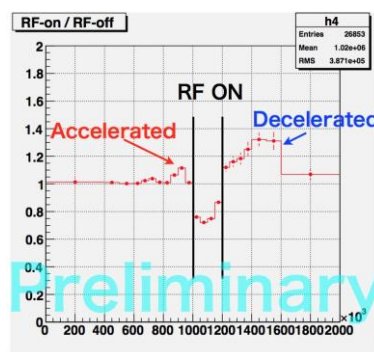


Fig. 2. The ratio between TOF spectra with RF ON and RF OFF. Accelerated and decelerated neutrons can be seen as excesses.

REFERENCES:

- [1] C. A. Baker, *et. al.*, Phys. Rev. Lett., **97**, 131801 (2006).
- [2] H. M. Shimizu, *et. al.*, Nucl. Instr. and Meth., **A 634**, 55-27 (2011).

D. Yamazaki, M. Nagano¹, F. Yamaga¹, K. Soyama, K. Yamamura¹, T. Oda² and M. Kitaguchi²

J-PARC Center, Japan Atomic Energy Agency

¹*Research Centre for Ultra-Precision Science and Technology, Osaka University*

²*Research Reactor Institute, Kyoto University*

INTRODUCTION: We have been developing supermirror devices for neutron beam focusing, free from chromatic aberration [1-3]. In order to focus large-size neutron beam into small spots, it is essential to develop “large acceptances” aspheric mirrors, i.e. large-size mirrors and/or “multiplexed” mirrors (stacked thin mirrors). In particular, multiplexed mirrors are compact and can be mounted in small interspaces.

One hurdle to fabricate a multiplexed mirror is to produce thin aspheric supermirror-substrates, i.e. figure surfaces of thin substrate of ~1mm in thickness into precise aspheric shape because the substrates absorb and scatter neutron beams. In this experiment, we fabricated elliptic surface of 0.5 $\mu\text{m-pv}$ in figure error and 0.2nm rms in surface roughness using the Numerically Controlled Local Wet Etching (NC-LWE) Technique and local low-pressure grinds. After the surface figuring, we have coated NiC/Ti ($m=4$) supermirror on the mirror substrate at JAEA.

In this experiment, we carried out a performance test of a single focusing supermirror on thin substrate on the CN3 beam line.

EXPERIMENTS: The focusing-mirror substrate was synthetic quartz of 100mm (L) x 35mm (W) x 1mm (T) in sizes and fabricated by the following for steps: (1) dip etching in hydrofluoric acid, (2) removal of altered surfaces by grinding, (3) damage-free surface figuring with NC-LWE, (4) removal of low-frequency roughness by grinding and (5) removal of high-frequency roughness by grinding [4]. We fabricated elliptic surface of 0.5mm-pv in figure error and 0.2nm rms in surface roughness After the surface figuring, we have coated NiC/Ti ($m=4$) supermirror on the mirror substrate at JAEA.

The elliptic mirror was designed for beam focusing at the BL10 “NOBORU” of J-PARC/MLF and ellipsoidal parameters are $a=3750.08\text{mm}$ and $b=24.64\text{mm}$, focal length is therefore 3750mm. This mirror is used on 12:1

condensing focal system.

The experiment was carried out on the CN3 beam line. We mounted, from the upstream, slit1, slit2, the elliptic mirror and a ³He detector as shown in Fig.1. The two slits were used to control size of a virtual beam source and beam divergence. We controlled the mirror alignment and observed focused beam profiles.

RESULTS: We could not find clear intensity peaks in any stage axis scans in the mirror alignments and therefore could not focus the neutron beam effectively. This result can be attributed to distortion of the mirror due to film stress. It is known that film stress of GPa order is to be introduced in the mirror coating process with an ion-beam sputtering machine. In this experiment, we coated both sides of the very thin substrate (1mm in thickness) in order to balance out the film stress. But it seems that the balancing out was not complete.

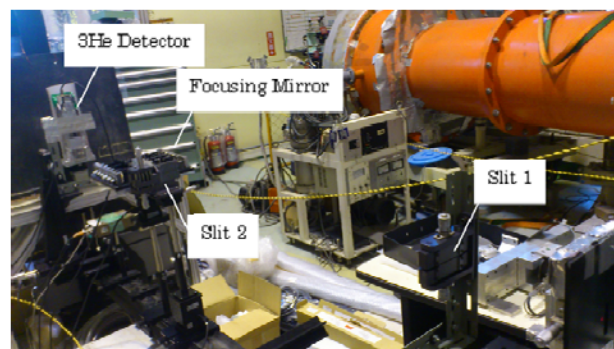


Fig.1 Experimental setup at the CN3 beam line.

REFERENCES:

- [1] K. Yamamura *et al.*, Annals of the CRISP 56/1 (2007) 541-544.
- [2] R. Maruyama *et al.*, Nucl. Instrum. Meth. A 600 (2009) 68-70.
- [3] K. Yamamura *et al.*, Opt. Express 17 (2009) 6414-6420.
- [4] M. Nagano *et al.*, Nucl. Instrum. Meth. A 634 (2011) S112-S115.

S. Tasaki, J. Miura, Y. Abe and M.Hino¹

Department of Nuclear Engineering, Kyoto University

¹Research Reactor Institute, Kyoto University

INTRODUCTION: As a matter wave, neutron forms a stationary wave in multilayer system under a certain condition. In such a stationary wave, the amplitude of neutron wave function takes definite value depending on the position in the multilayer. If we insert an absorbing layer for neutron, such as Gd layer, into the multilayer, the neutron reflectivity changes depending on the amplitude of the wave function at the position of the absorbing layer. By analyzing the reflectivity, the amplitude of neutron wave function in the multilayer can be estimated. In the present study, we studied a Fabry-Perot multilayer consisting of Ni and Ti, where the neutron wave function forms stationary wave under resonant tunneling condition. We fabricated a few Fabry-Perot mirrors with absorbing layer at different positions, made measurement of neutron reflectivity and analyzed to estimate the neutron wave function in the multilayer.

EXPERIMENTS: In Fig. 1, an example of optical potential for neutron is presented. The material with low-optical potential (Ti) is sandwiched by the material with high-optical potential. If a neutron whose normal

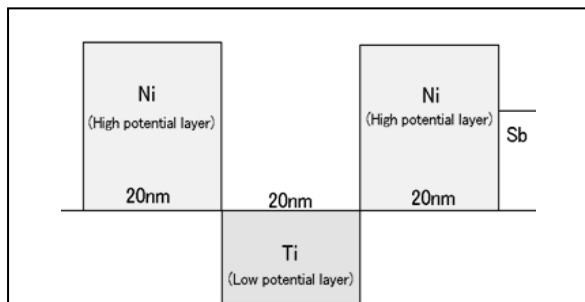


Fig.1 An example of neutron optical potential of a Fabry-Perot mirror.

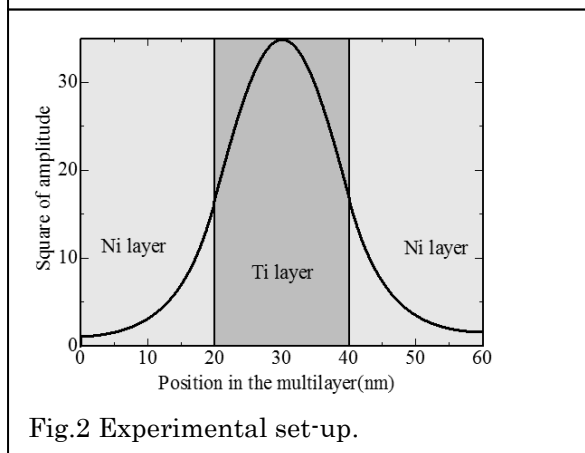


Fig.2 Experimental set-up.

wavelength is equal to the thickness of the Ti layer, because of the enhancement of neutron wave function in the Ti layer by reflecting by the Ni layers at both sides, a stationary wave is formed in the Ti layer as shown in Fig.2. In Fig.2, horizontal axis and vertical axis represent the position in the multilayer and the square of the wave function, respectively.

The sample Fabry-Perot mirrors with absorbing material were fabricated on Si wafers with vacuum evaporation. Neutron reflectivity measurements were performed at CN-3 beam port of KUR, when the operating power of 5MW.

RESULTS: Figure 3 shows examples of measured neutron reflectivity. The left and right figure correspond to the Fabry-Perot multilayer without and with absorbing layer, respectively. Black circles with error bar represent the measured reflectivity, and the solid lines stand for calculated. Because of low resolution (about 10%), the reflectivity dip due to the resonant tunneling is smeared. The calculated results, however, agree well with the measured results.

From these results, we estimated the depth of the dip δ and plotted $(1-\delta)$ as a function of the position in Fig. 4. The square of amplitude of the wave function is also plotted (broken line) in the same figure. As shown in Fig. 4, $(1-\delta)$ correspond to the square amplitude of the wave function.

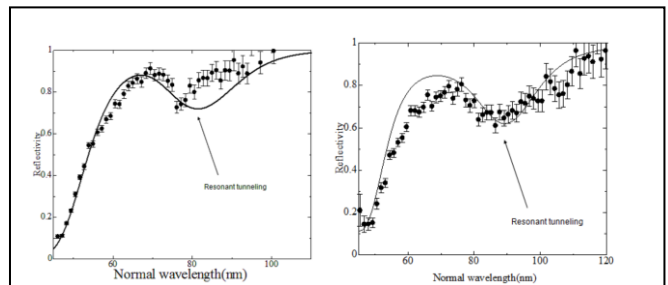


Fig.3 Neutron reflectivity of the Fabry-Perot multilayers without (left) and with (right) absorbing layer.

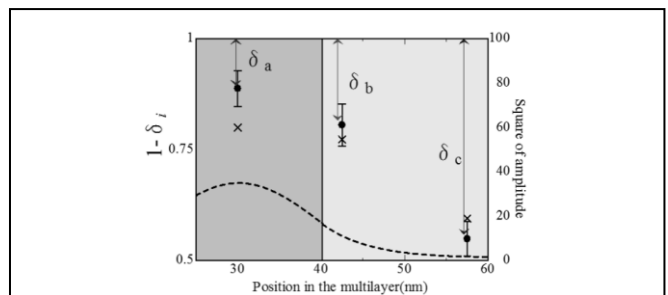


Fig.4 The depth of the dip d as a function of the position of absorbing layer in the multilayer.

CO1-7 Improvement of KUR-IBS as a Large-Scale Neutron Supermirror Fabrication Machine

M. Hino, T. Oda¹, M. Kitaguchi and Y. Kawabata

Research Reactor Institute, Kyoto University

¹Department of Nucl. Eng., Kyoto University

INTRODUCTION: Supermirror is most important key component of neutron guide tube. The total length of neutron guide tube is, in general, longer than 10 m. When we fabricate neutron guide tube, the size of deposition area is very important. Ion beam sputtering (IBS) technique enables us to fabricate smooth layer structure with sharp edge and we have succeeded in fabricating $m > 5$ supermirrors and very small d-spacing multilayer [1]. The maximum substrate area at our KUR-IBS machine was limited to 200 mm in diameter. On the other hand, the maximum substrate area at JAEA is 500 mm in diameter. It is enough large to fabricate neutron guide tube and they are producing a lot of supermirrors for J-PARC project [2]. In FY2011, Kyoto University and KEK started to construct a new beam line for neutron spin echo (NSE) spectrometers at BL06 at J-PARC/MLF. The NSE spectrometers are called "VIN ROSE" and it has been developed at C3-1-2-2(MINE1) beam line at JRR-3 reactor. We have designed the BL06 beam line and start to fabricate supermirrors for the guide tube by using the KUR-IBS machine. The total length of the guide tube is about 29 m. It is really big task for us to fabricate all supermirror components; however, we are going to do it because KURRI has a feasible future program: Promotion of Leading Research toward Effective Utilization of Multidisciplinary Nuclear Science and Technology. It is, fortunately, accepted as one of "Japanese Master Plan of Large Research Projects: A Table of 43 Selected Projects" at FY2010 and FY2011. We consider that there is a big demand to improve manufacturing ability of neutron guide in house. We will gain lots of valuable experience by constructing the VIN ROSE beam line and the experience contributes to improve neutron guide installed at KUR, such as E-3, and to construct new neutron facility for KURRI. In this study, we show progress of fabrication of large scale supermirror with high performance.

EXPERIMENTS: Figure.1 shows photograph of new substrate holder for fabrication of the BL06 guide tube at J-PARC. The diameter of substrate holder is limited by size of process vacuum chamber. The substrate holder and attachments were developed at the

workshop in KURRI. Figure 2 shows reflectivity by NiC monolayer and $m=2.5, 3$ supermirror on the silicon wafer. The wafer is placed on three points, top, center, bottom on the substrate holder. The center means middle of circle (substrate holder), top and bottom is about 200 mm outer from the center. The measurement was carried out at Time-Of Flight (TOF) instrument installed at CN-3 beam port. These reflectivities at all points were high and almost reproduced by the theoretical ones. We succeeded in fabrication of large scale neutron supermirror with high reflectivity for real neutron guide. As the next step, we are seeking best sputtering condition to increase fabrication yield with high quality.

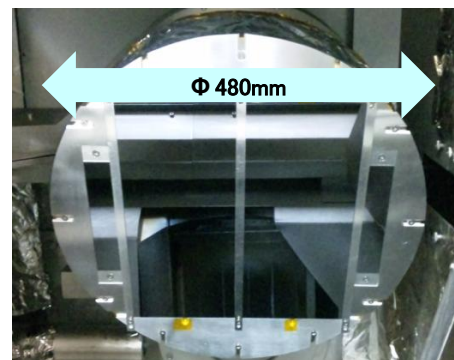


Fig.1. The photograph of new substrate holder in which diameter is 480 mm and silicon wafers placed at the substrate holder in KUR-IBS.

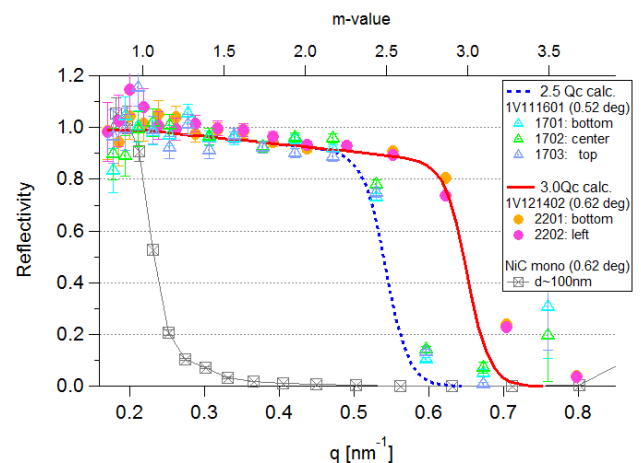


Fig.2. Measured and theoretical reflectivity of NiC monolayer, $m=2.5, 3$ supermirror deposited on silicon wafers.

REFERENCES:

- [1] M.Hino, *et al.*, Nucl.Inst.Meth., A **574** (2004)292.
- [2] R.Maruyama, *et al.*,Physica B **385-386**(2006)1256, *ibid.*, in this progress report.

CO1-8 Performance Test of Supermirrors for a Guide Element Fabricated in the JAEA

R. Maruyama, T. Oda¹, M. Hino², M. Kitaguchi², D. Yamazaki, H. Hayashida, and K. Soyama

J-PARC Center, Japan Atomic Energy Agency

¹*Graduate School of Engineering, Kyoto University*

²*Research Reactor Institute, Kyoto University*

INTRODUCTION: Neutron supermirror is one of the most useful optical devices for transporting, bending, and focusing neutron beams. The thickness of the layers needs to be decreased and the number of the layers increased to extend the effective critical angle of a supermirror. The effective critical angle of the supermirror is characterized by the ratio m of the critical angle of the supermirror to that of natural nickel. The development of high-performance supermirror is important in neutron experiments since it leads to a considerable increase in available neutron intensity. The neutron reflectivity of the fabricated supermirrors needs to be measured in order to keep and improve the performance of our fabrication system based on ion-beam sputtering (IBS) system and to confirm the surface roughness of the substrate.

EXPERIMENTS: Neutron supermirrors were fabricated by using an IBS system with dual bucket Ar^+ ion sources, installed in the Japan Atomic Energy Agency. Test fabrication of NiC/Ti supermirrors [1-3] with $m=4$ for a guide element were performed using glass substrates (TEMPAX Float[®]). The layer sequence was designed by using the algorithm proposed by Hayter and Mook [4]. The Total number of layers was 1201. Neutron reflectivity measurement was performed on a versatile instrument of CN-3 at the research reactor, KUR, in the Research Reactor Institute, Kyoto University. Top view of the experimental setup is shown in Fig. 1. A polychromatic pulsed beam with a wavelength longer than 0.2 nm is used for the measurement. The wavelength spread is estimated to be less than 5%. The incident beam was collimated by a pair of horizontal slits to a divergent angle of 1.4 mrad.

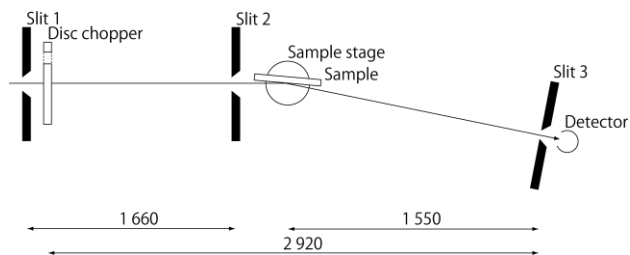


Fig. 1. Top view of experimental setup for neutron reflectivity measurement on a versatile instrument of CN-3 in the research reactor, KUR (unit: mm).

RESULTS and SUMMARY: Measured neutron reflectivity profiles are shown in Fig. 2. The deposition of the supermirrors is completed as we designed since the critical angle coincides with $m=4$ for each sample. The rapid decay in reflectivity is observed at the momentum transfer range higher than 0.215 nm^{-1} ($m=1$). The reflectivities at the critical angle are 40% for all of the samples, which is lower than the expected value of 60%. This can be attributed to the surface roughness of the glass substrates since it is known that the surface roughness of this kind of glass substrates depends on the details of the production such as the composition of glass and the floating process. This result implies that the process to check the surface roughness before deposition needs to be established.

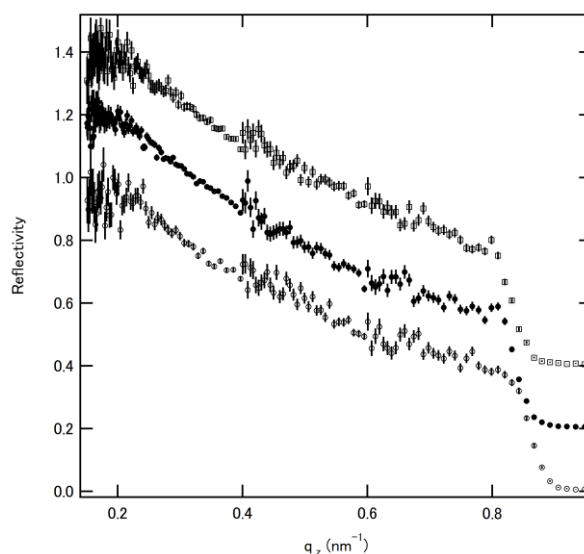


Fig. 2. Measured neutron reflectivity profiles of the supermirrors fabricated in the JAEA. The base reflectivities shown in closed circles and open squares are shown to be shifted upward by 0.2 and 0.4 units, respectively.

ACKNOWLEDGEMENTS: The authors (R.M., D.Y., H.H., and K.S.) would like to express our sincere gratitude for all the people who supported us in our hard days after the earthquake.

REFERENCES:

- [1] J. Wood, Proc. SPIE, **1738** (1992) 22.
- [2] K. Soyama, Ph.D. thesis, Kyushu University, 1999.
- [3] M. Hino *et al.*, Nucl. Instrum. Methods Phys. Res., A **529** (2004) 54.
- [4] J. B. Hayter and H. A. Mook, J. Appl. Crystallogr., **22** (1989) 35.